ScienSage

Journal of Advanced Scientific Research

Available online through http://www.sciensage.info

ISSN
0976-9595
Research Article

ELECTRICAL AND STRUCTURAL CHARACTERIZATION OF ANNEALED TIN OXIDE THICK FILMS PREPARED BY SCREEN PRINTING TECHNIQUE

Rohit M. Nikam*[1], Kailas H. Kapadnis[2], Ratan Y. Borse[3]

[1]*Department of Chemistry, M. J. M. ACS College, Karanjali, Tal- Peth, Nashik, Maharashtra, India*

[2]*Department of Chemistry, L. V. H. ACS College, Panchavati, Nashik, Maharashtra, India*

[3]*Department of Physics, M. J. M. ACS College, Karanjali, Tal- Peth, Nashik, Maharashtra, India*

**Corresponding author: rohitnikam9@rediffmail.com*

ABSTRACT

Thick films of tin oxide (SnO_2) were prepared by Standard Screen printing method on glass substrates. Thick films of tin oxide were annealed at 500°C for 5 hrs. in muffle furnace. Electrical characterization was performed in static system. Electrical study was performed with respect to resistance (R), activation energy (ΔE) at low and high temperature in terms of Arrhenius plot and temperature coefficient of resistance (TCR). Structural parameters of thick films of tin oxide (SnO_2) were performed by scanning electron microscopy, energy dispersive spectroscopy, X-ray diffraction, fourier transform infra-red and UV-visible to study surface morphology and surface area, elemental detection in qualitative and quantitative approach, crystalline Phases of films and crystallite size of tin oxide phase material, vibrational and optical modes in terms of absorbance and band gap respectively.

Keywords: Screen printing method, Electrical characterization, Structural parameters, Resistance, Band gap etc.

1. INTRODUCTION

There are numerous methods have been developed to fabricate thin and thick films in the material science. From the last fifty years, several methods have been investigated and developed day by day. The methods include spray pyrolysis evaporation, chemical vapor deposition, sol gel technique, magnetron sputtering pulsed laser deposition and screen printing technique [1]. Among all, screen printing is simple and low cost method to fabricate thick films for different applications like solar cells, optical devices, transistors and gas sensors. SnO_2 material is used for oxidation catalyst [2-5]. Tin oxide is mostly used material for different applications because of its high sensitivity, chemical inertness, inexpensive material, material stability and relatively low operating temperature. Tin oxide is oxygen deficient n-type semiconductor [6]. It is colorless, diamagnetic and amphoteric solid with high melting point and boiling point. The properties and applications of nanomaterial SnO_2, TiO_2 and ZnO have been widely investigated and studied in terms of electric, gas sensing and structural basis [7-9]. Structural, absorption and optical study was studied for thin and thick films prepared by different methods [10-12].

Absorption spectra of tin oxide nanoparticles obtained in UV-visible region show blue shift in the absorption edge at 268 nm as compared to bulk. The band gap value was 4.66 eV. This blue shift was useful in gas sensing applications [13]. The reported band gap of tin oxide was 3.6 eV [14]. We have performed electrical study using static electrical set up and structural parameters such as XRD, SEM, EDAX, FTIR and UV-visible were characterized to study crystallite phase analysis, surface morphology and elemental detection, vibrational and optical analysis.

2. MATERIAL AND METHODS

2.1. Thick Film Preparation

Tin-oxide (SnO_2) solid thick films were prepared on glass substrate with particular size by using standard screen-printing technique [15-20]. The analytical grade tin oxide (SnO_2) powder (99.99 % pure) was weighed. The SnO_2powder was mixed and crushed thoroughly with glass frit composition which acts as permanent binder and ethyl cellulose acts as a temporary binder. The mixture was then mixed with butyl carbittol acetate as organic vehicle to form the paste. The paste was then screen printed onto the surface of glass substrate in mask position. The detail of the technique was as

described [17]. Thick films were dried under ordinary visible lamp of power 200 watt for 2-3 hrs. followed with annealing into muffle furnace, dried under air atmosphere at 500°C for 5 hrs. After preparation, SnO_2 thick films were subjected to electric and structural charactrization.

2.2. Electrical characterization

The resistance of the solid thick films of tin oxide sample was measured by using half bridge method at different temperatures in glass dome as described in following Fig. 1. Variable D.C. power supply (APLAB 0-30V, 2A) was employed to enable the user to choose the required voltage; the voltage across the standard reference resistance was measured by digital multimeter. The thick films of tin oxide samples were heated slowly to avoid any thermal runway. At the selected interval of temperature, voltage across the reference resistance was noted. In the paper five thick films of tin oxide is under consideration for electrical study. In electrical study, resistance, activation energy and TCR have been evaluated with increase in temperature. The resistance of thick film samples of tin oxide was calculated by using the Equation 1 [21],

$$R_F = R_{ref}\,[V_{supply}/V_{ref}] \quad (1)$$

Where, R_F-Resistance of thick film,R_{ref} -Resistance of Standard reference resistance,V_{supply} Applied voltage,V_{ref} -Reference voltage across standard resistance.

The activation energy (ΔE) is calculated with following equation 2 [21],

$$R_T = R_0 e^{-\Delta E/kT} \quad (2)$$

Where, R_T is resistance at T, R_0 is resistance at T_0, ΔE is activation energy and k is Boltzmann constant over a limited temperature range.

And TCR is calculated with following equation 3 [21],

$$TCR = \frac{1}{R_0}\frac{\Delta R}{\Delta T} \times 10^6 \frac{ppm}{^\circ K} \quad (3)$$

Where, ΔR is change in resistance between T_1 and T_2, ΔT is temperature difference between T_1 and T_2, R_0 is initial resistance of film sample

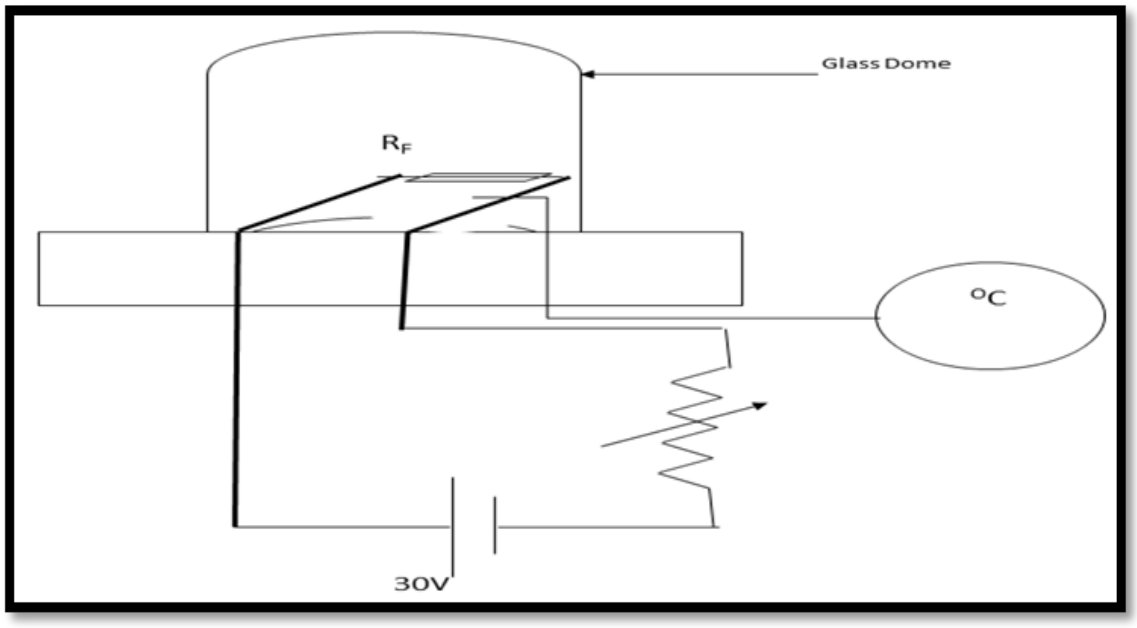

Fig. 1: A set up of block diagram for static system for measurement of resistance, ΔE and TCR

2.3. Structural characterization

Using X-ray diffraction (Miniflex Model, Rigaku, Japan) analysis from 20-80, 2θ was carried out to determine the crystalline phases of the SnO_2 films samples. The crystallite size along the XRD spectrum of tin oxide was calculated by using the Scherer formula [18].

$$D = \frac{0.9\lambda}{\beta COS\theta} \quad (4)$$

Where, D is average crystallite size, λ is x-ray wavelength, β is FWHM and θ is peak position.

The microstructure and chemical composition of the films were obtained using a scanning electron microscope (Nova nano SEM NPEP303) coupled with an energy dispersive spectrometer (EDS JEOL, JED-2300, Germany). FTIR is useful technique as qualitative and quantitative tool for organic and inorganic samples.

It is useful for solids, liquids and gaseous samples and measures the wide range of wavelengths in IR spectra that are absorbed by the material. The FTIR was done by following standard method of solid phase KBr pellet technique. The FTIR spectrum was recorded at room temperature for pure SnO_2 in IR Affinity-1 Shimadzu FTIR Instrument. A small amount of 2 to 5 mg sample powder was mixed in approximate 250mg-300 mg Potassium Bromide (KBr) of spectroscopic grade purity to form clear transparent proper 13mm circular pallet or disc with 1mm thickness when mixture was pressed in KBr Press Model M-15 at a pressure of about 5×106 Pa in an evacuated die. FTIR spectra were recorded between 400 cm^{-1} to 4000 cm^{-1} consists of transmittance at different spectral resolution of 2 cm^{-1} and taking 32 scans for each sample. UV spectroscopy is an intense non-destructive testing technique for exploring the properties of semiconductor nanomaterial. Absorbance may depend on nature of surface, oxygen deficiency, band gap and impurity centers.

3. RESULT AND DISCUSSION

3.1. Electrical study of tin oxide thick films

The electrical study was considered for five thick films of tin oxides. In this study resistance, activation energy and temprature coefficient of resistance was plotted against temprature. Fig. 2 shows the variation in resistance of tin oxide thick films. The variationin sample to sample wasobserved due to different thickness of film, as thinner the film larger the electrical resistance of the thick film and *vice-versa* [22].

Fig. 3 shows the graphs of two sections of linear region, one is for higher temperature region and another is for lower temperature region. The activation energy in the low temperature region is always less than the activation energy in the high temperature region because material passes from one conduction mechanism to another as illustrated [23].

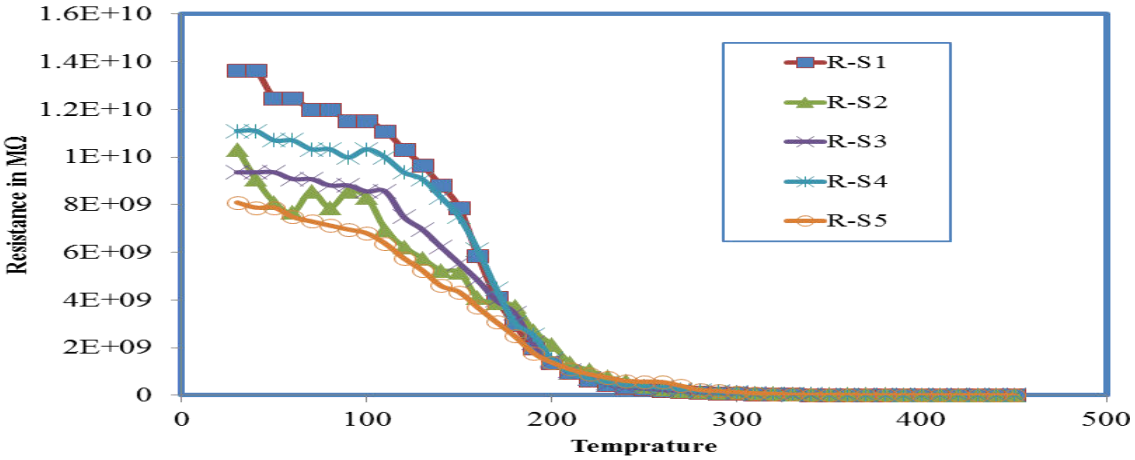

Fig. 2: Variation in resistance of tin oxide films with temperature

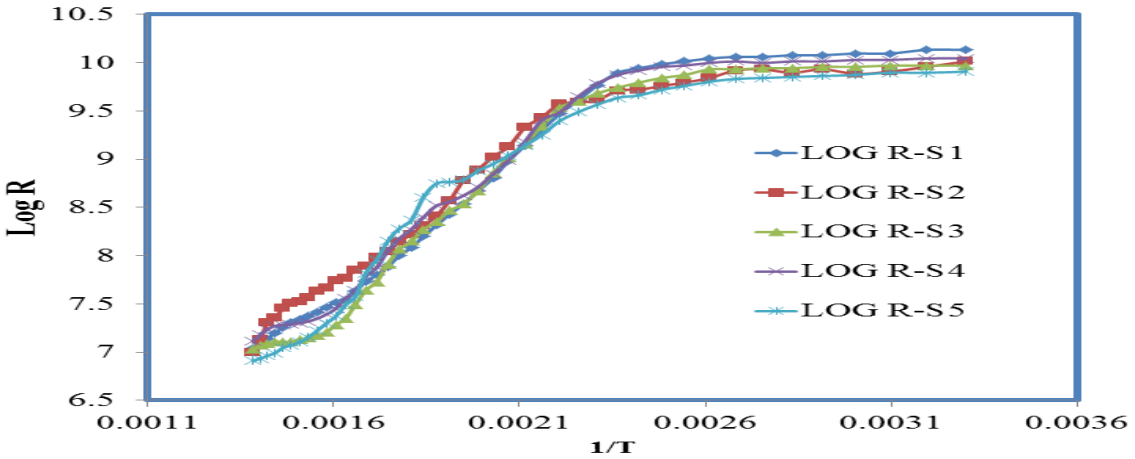

Fig. 3: Arrhenius plot at low and high temperature region of tin oxide films

In TCR graphs, there is increase in temprature with TCR is observed initally and fall in TCR is observed after with increase in temprature indicating negative coefficient of temprature. This is implication of semiconducting behaviour. This result may be attributed to the degree of crystallinity with the annealing temprature [21].

In sample to sample variation for resistance, activation energy and TCR, nature of increase and decrease are as shown in following figs. 5-7. S1 sample has most resistance while S5 sample has least resistance. The activation energy has two distinct natures, one is for low region and another is for high region. Upon comparison, activation energy in high region is high for S5, while low for S1 sample. Activation energy is high for S1 and becomes approximately saturated or approximate constant value up to S5. The TCR value is maximum for S1 and minimum for S5 tin oxide solid thick film.

Table 1: Variation in sample to sample for tin oxide thick films

					Activation enengy (ΔE)	
	Sample	Resistance (ΩM)	T.C.R	T.C.R	LTR	HTR
Pure SnO_2	S1	252087	0.02312	0.08186	0.131742	0.460904
	S2	211863	0.02216	0.0489	0.09315	0.495505
	S3	163887	0.008856	0.05037	0.104348	0.510147
	S4	233123	0.008445	0.06465	0.10737	0.507665
	S5	174109	0.014216	0.041055	0.10893	0.704626

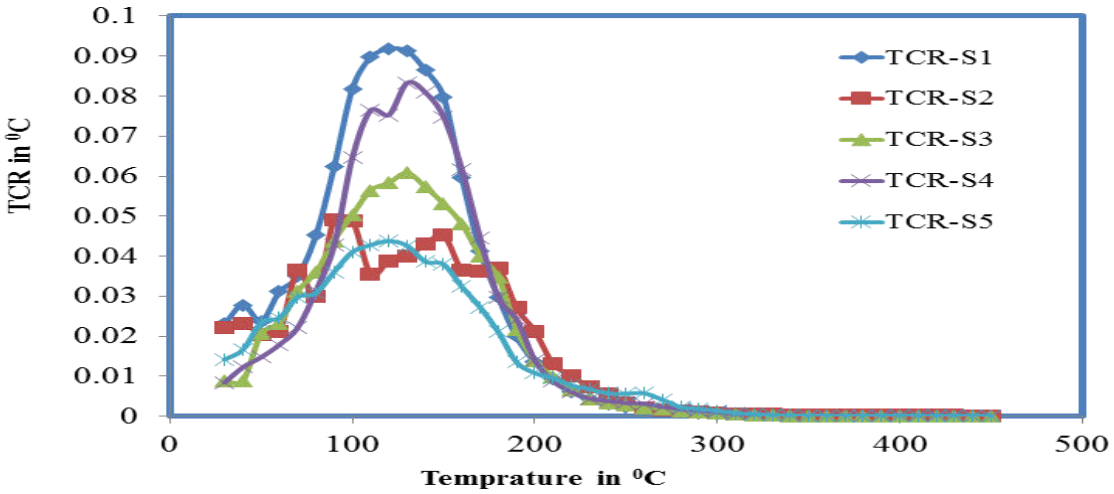

Fig. 4: variation in TCR of tin oxide films with temperature

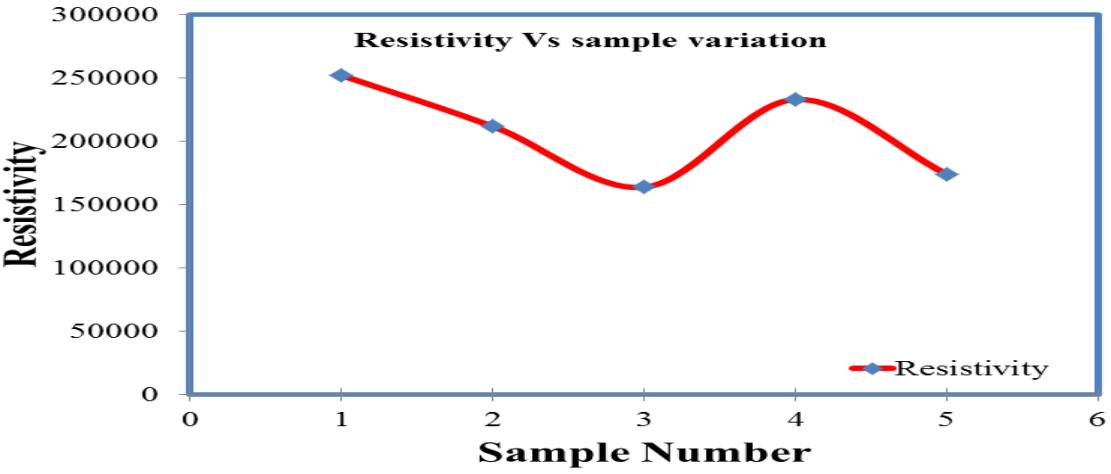

Fig. 5: Sample variation in resistance of tin oxide films

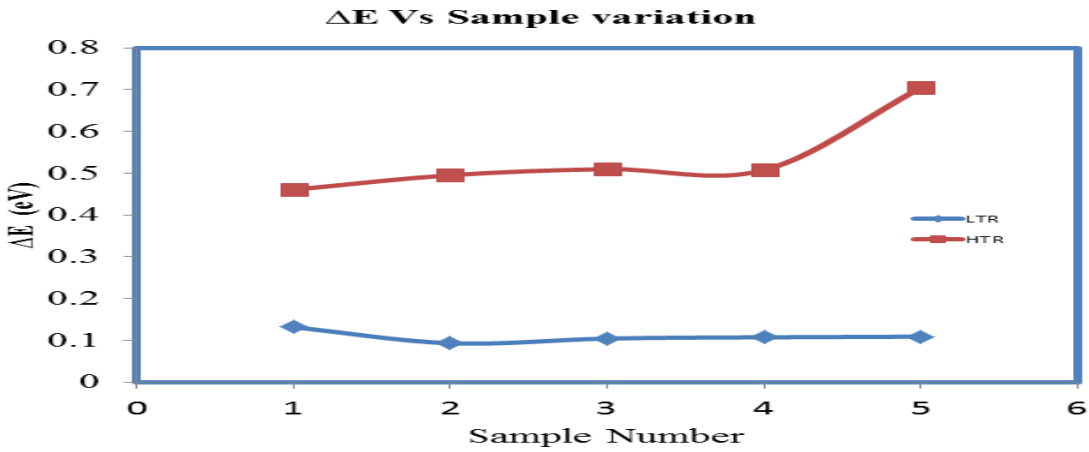

Fig. 6: Variation in Arrhenius energy of tin oxide films

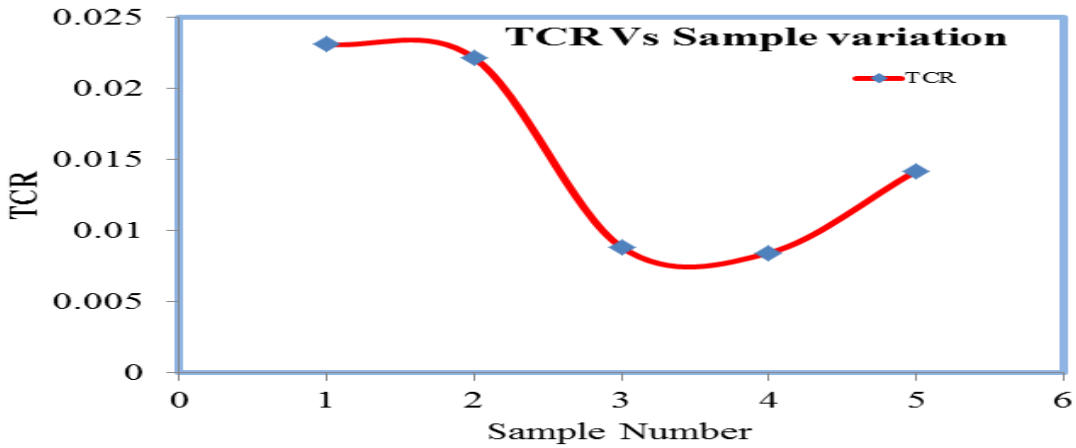

Fig. 7: Sample variation in TCR of tin oxide films

3.2. Structural study of tin oxide thick films

3.2.1. X-ray diffrection (XRD) analysis

XRD analysis of dried powder of thick films of tin oxide annealed at 500°C for 5 hrs is used for confirming the size of nanoparticles. The diffraction peaks located at different peak position are in good agreement with tin oxide tetragonal phase structure indicating poly-crystaline nature. Observed peaks are sharp and crystalline. All peaks are well matched with JCPDS card No. 41-1445 [24]. The intensity peak (101) at peak position 26.66 was observed to be very strong and intense in the multi-peakplot (Fig. 8). The calculated crystal size and lattice parameters are as shown in Table-2.

3.2.2. Scanning elecctron Microscopy (SEM) and elemental detection

The SEM micrograph image indicate that the particles have non-uniform size with high degree of agglomeration. The apperance of some of particles are irregular and non-uniform [25]. They are gathered together into bigger particles parting some pores between which make useful to them for various applications. The SEM micrograph exhibit a clear surface with a few microvoids. This voids are also useful in optoelectronic devices and gas sensing applications. The avarage grain size of following sem micrograph was 46 nm. Fig. 9 is the SEM micrograph of tin oxide powder fired at 500°C for 5 hrs with magnification of 50000x. The instrumental parameters, accelerating voltage, magnification range and spot size were used to control and obtain the SEM image of tin oxide [25].

The elemental detection of tin oxide powder is as shown in Fig. 10. The EDAX spectrum is the graph of cps/eV and keV. The presence of tin and oxygen is well ascertained and defined qualitatively and quantitatively in terms of atomic and weight percentage. The values are illustrated in table 3. EDAX indicates the presence of both elements.

Table 2: Crystal parameters and particle size of tin oxide

2θ (deg)	F.W.H.M (deg)	d value(Å)	Crystallite size (nm)	Plane(h k l)
26.66	0.669	3.340	12.20	110
33.94	0.663	2.639	12.52	101
51.84	0.619	1.762	14.26	211

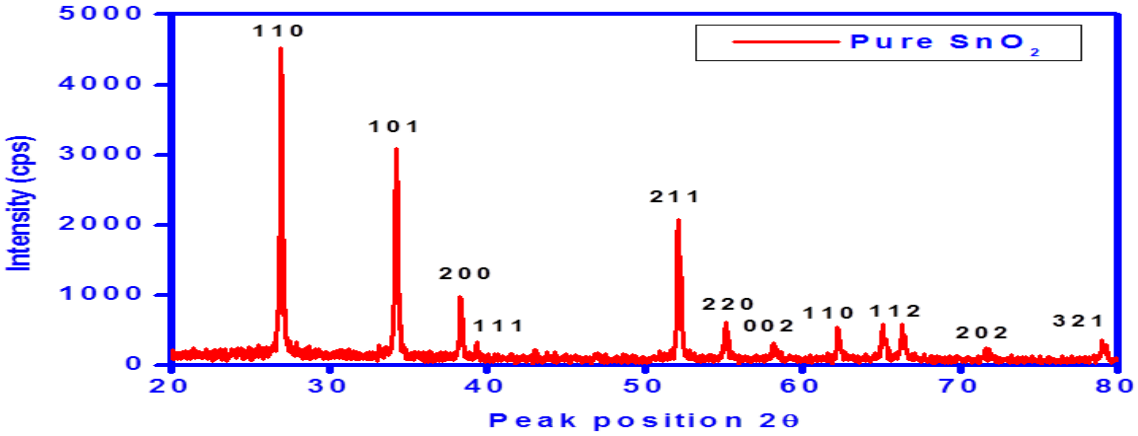

Fig. 8: The XRD pattern of tin oxide fired at 500°C

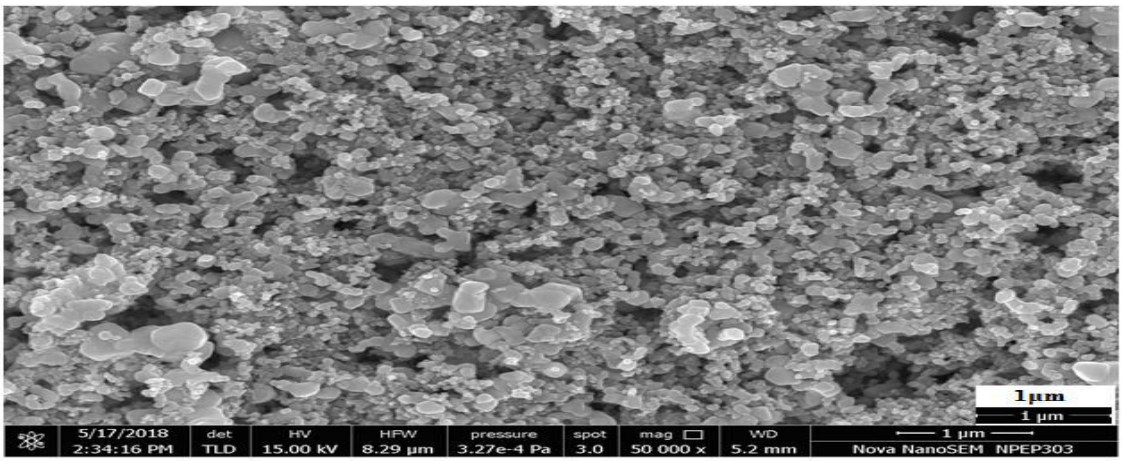

Fig. 9: SEM micrograph of tin oxide fired at 500°C

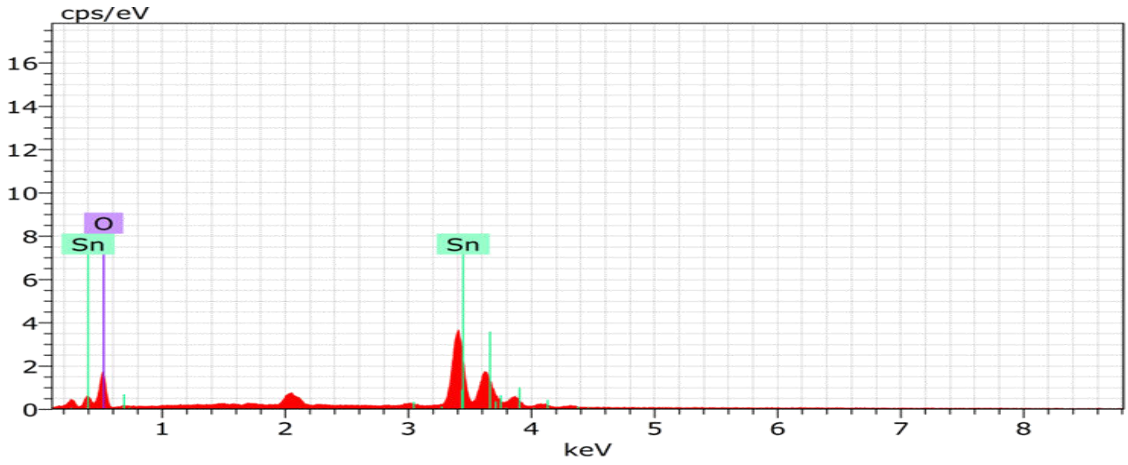

Fig. 10: EDAX spectrum of tin oxide fired at 500°C

Table 3: Quantitative elemental analysis

Element	Atomic number	Series	Wt. %	At. %
Sn	50	L	71.73	25.49
O	8	K	28.27	77.51
		Total	100.00	100.00

3.2.3. FTIR Study

Fourier transform infra-red spectroscopy is an effective analytical instrument for collecting information about functional groups and nature of covalent bond over a broad wavenumber region.

An intense broad band at 617 cm^{-1} attributed to Sn-O bond in SnO_2 [26-27]. The frequencies observed at 1633 cm^{-1} and 1381 cm^{-1} is attributed to presence of water molecules [28]. The frequencies observed at 2924 cm^{-1} and 3446 cm^{-1} is due to O-H stretching vibration.

3.2.4. Optical Study

The optical absorption edge of tin oxide annealed at 500°C for 5 hrs was 282 nm. The maximum absorbance at this data point was 0.93403 nm as indicated in Fig.12.

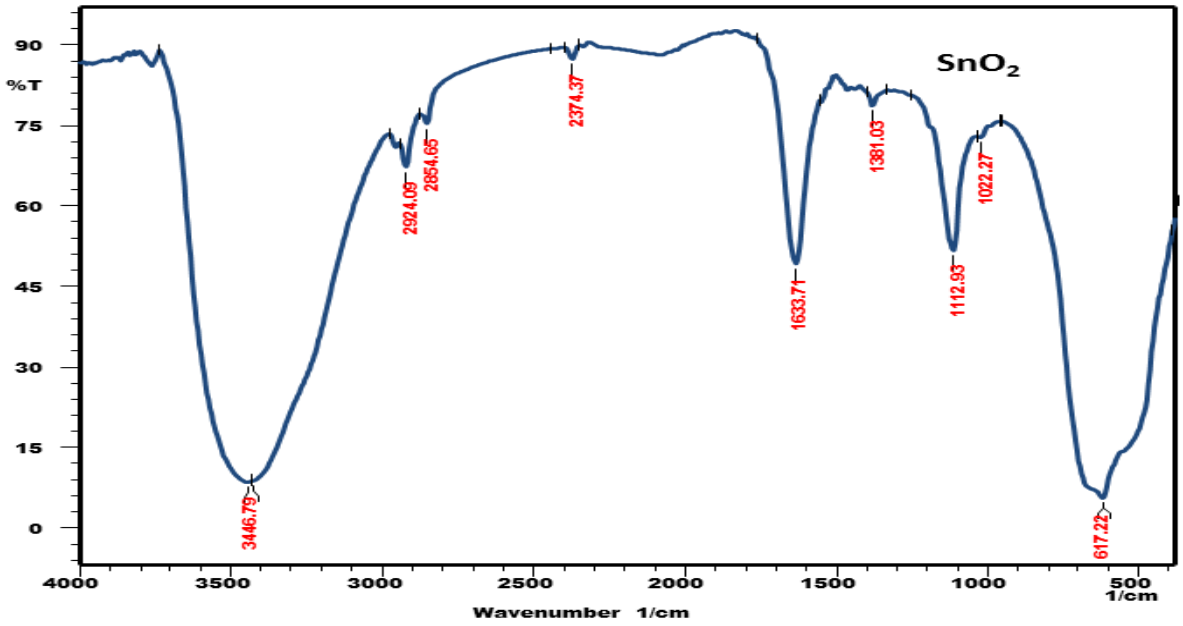

Fig. 11: FTIR pattern of tin oxide fired at 500°C

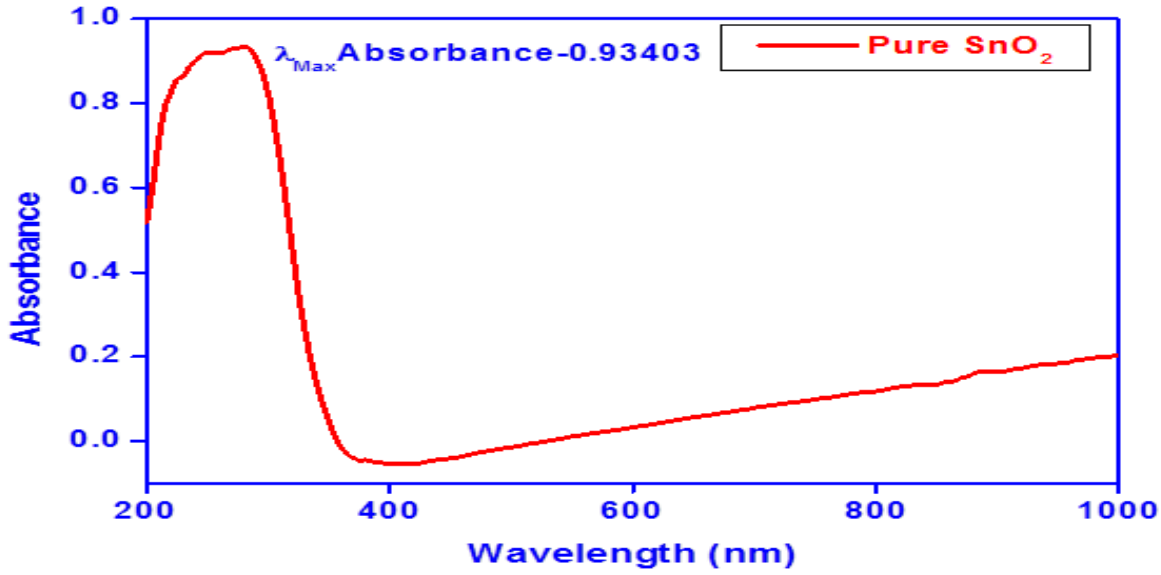

Fig. 12: Absorbance spectrum of tin oxide nanostructure fired at 500°C

The band gap of SnO_2 was calculated following tauc's equation 4 [29],

$$(\alpha h\upsilon)^{1/n}=A(h\upsilon-E_g) \quad (4)$$

Where E_g is the band gap, A is energy independent constant, n=1/2 for direct band gap of material, α is absorption coefficient, hυ is incident photon energy where h is Planck's constant and υ is frequency. The extrapolated linear portion to horizontal axis of the tauc's plot gives value of band gap. The band gap for thick film of tin oxide material was around 3.77 eV which attributes a slight variation in blue shift with literature value 3.6 eV [27, 29]. This insignificant change is due to reduction in particle size from bulk material as films were heated at high temperature.

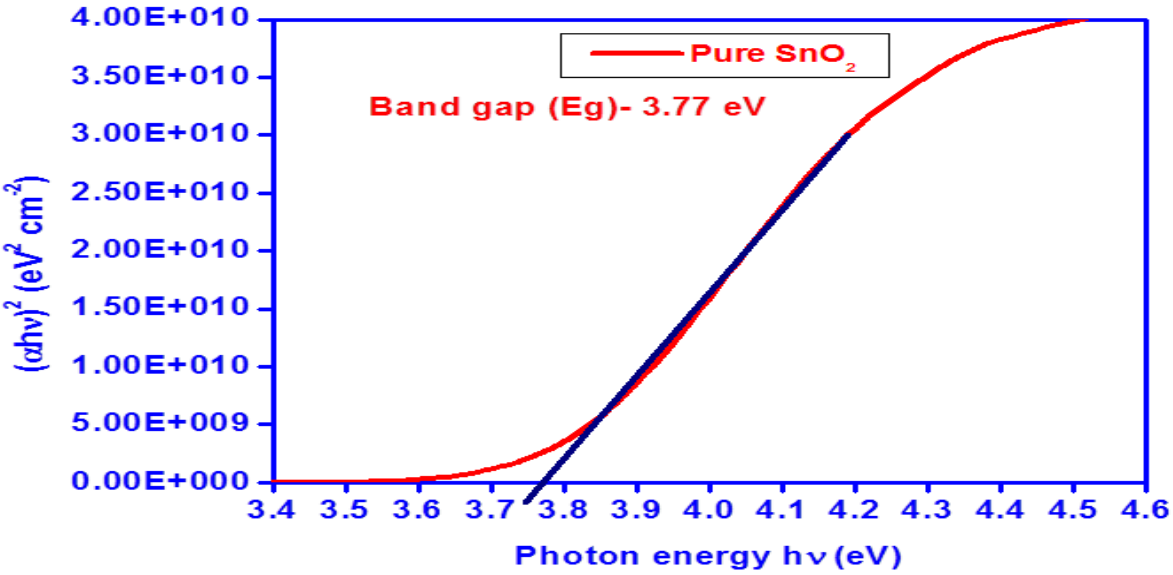

Fig. 13: Band gap of tin oxide nanostructure material fired at 500°C

4. CONCLUSION

The thick films of tin oxide were successfully prepared by standard screen printing technique. The electrical study of tin oxide thick films was investigated for resistance, activation energy (ΔE) and temperature coefficient of resistance (TCR) with temperature. The structural parameters like X-ray diffraction suggest polycrystalline nature with tetragonal phase of tin oxide. Average crystallite size of XRD spectrum was 13 nm. The Scanning electron microscopy reveals about grain size which is 46 nm. The EDAX spectrum reveals the presence of tin oxide in proper elemental composition. The FTIR spectrum confirms the frequencies of tin oxide material over a broad region of transmittance. The absorption edge at 282 nm confirms the bang gap of tin oxide at 3.77 eV.

5. REFERENCES

1. Shukla T. *Journal of sensor technology*, 2012; **2:**102-108.
2. Krishnan B, Nampoori VPN. *Bulletin of material science,* 2005; **28(3):**239-242.
3. Guidi V, Butturi MA, Carotta MC, Cavicchi B, Ferroni M, Malagu CM, et al. *Sensors and actuators B*, 2002; **84(1):**72-77.
4. Joseph B, Gopalchandran KG, Manoj PK, Koshy P, Vaidyan VK. *Bulletin of material science,* 1996; **22(5):**921-926.
5. Jaydev DN, Sainkar SR, Karekar RN, Aiyer RC. *Thin solid films*, 1998; **325(1):**254-258.
6. Borse RY, Sensors and transducers principles and investigation, 1st ed. ISBN: 978-81-8435-052-4: Adhyayan publishers & distributors (New Delhi); 2008.
7. Borse RY, Garde AS. *Sensors and Transducers,* 2009; **111(12):**155-165.
8. Li J, Yaan H. *Crystal research technology*, 2017; **52(12):** 1-9.
9. Patil AV, Dighavkar CG, Borse RY, Sonawane SK.*Invertis Journal of Science and Technology*, 2010; **3 (4):**207-214.
10. Bhatnagar M, Kaushik V, Kaushal A, Singh M, Mehta BR. *AIP advances*, 2016; **6:**095321, 1-11.

11. Demiryont H, Nietering KE. *Solar Energy*, 1989; **19:**79-94.
12. AlamM, Anees A, Ansari, Shaik MR, Naser M. Alandi. *Arabian Journal of Chemistry*, 2013; **6:**341-345.
13. Shukla T. *Journal of sensor technology*, 2012; **2:**102-108.
14. Watson J. The tin oxide gas sensors and its applications, *sensors and actuators* 1984; **5(1):**29-42.
15. Ansari SG, Boroojerdian P, Kulkarni SK, Sainkar SR, Karekar RN, Aiyer RC. *Journal of Materials Science: Materials in Electronics*, 1996; **7:**267-270.
16. Prudenziati M, Morten B. *Sensors and Actuators*, 1996; **10:**65-82.
17. Harper CA, Handbook of Thick film hybrid Microelectronics; (NY) Mc Graw Hill Book Co. 1974.
18. Kiran J, Pant RB, Laxmikumar ST.*Sensors and Actuators, B,* 2006; **113:**823-829.
19. Nimal AT, Kumar V, Gupta AK. *Indian Journal of pure and applied physics*, 2004; **42:**275-278.
20. Patil LA, Wani PA, Amalnerakar DP. *Mater. Chem. Phys*, 1998; **55:**79-83.
21. Dighavkar CG, Patil AV, Borse RY, Patil SJ. *Optoelectronics and advanced materials-rapid communication*, 2009; **3(10):**1013-1017
22. Suhendi E, Novia H, Dani GS. *Proceedings of the third international conference on mathematics and natural science (ICMNS)* 2010; **1:**600-607.
23. Ahmed FIS, Battisha IK, El-Raffay MM. *Indian Journal of pure and applied Physics*, 2005; **43:**446-458
24. Al-Saadi TM, Hussain BH, Hasan AB, Shehab AA. *Energy Procedia*, 2019; **157:**457-465.
25. Omar KA. *ARO, The scientific journal of koya university*, 2013; **1:(1)**17-21,
26. Zhang J, Gao L.*Inorg. Chem. Commun*, 2004; **7:**91-93
27. Tan L, Wang L, Wang Y. *Journal of nanomaterials*, 2011; article ID 529874**2011:**1-11
28. Tripathi A, Shukla RK. *Bulletin of Material Science,* 2014; **37(3):**417-423.
29. Sagadevan S, Podder J. *Material Research*, 2016; **19(2):**420-425.